Journal of Solid State Chemistry **143,** 24–32 (1999)
Article ID jssc.1998.8061, available online at http://www.idealibrary.com on IDEAL®

Low-Temperature Polymorphism in Tungsten Trioxide Powders and Its Dependence on Mechanical Treatments

E. Cazzanelli,* C. Vinegoni,† G. Mariotto,† A. Kuzmin,‡ and J. Purans‡

*Istituto Nazionale per la Fisica della Materia and Dipartimento di Fisica, Università della Calabria, 87036 Arcavacata di Rende, Cosenza, Italy;
†Istituto Nazionale per la Fisica della Materia and Dipartimento di Fisica, Università di Trento, 38050 Povo, Trento, Italy; and
‡Institute of Solid State Physics, University of Latvia, LV-1063 Riga, Latvia

Received April 12, 1998; in revised form October 14, 1998; accepted October 19, 1998

The polymorphism of WO_3 powder samples, resulting from mild mechanical treatments and from temperature changes between 30 K and room temperature, has been investigated by using Raman spectroscopy and X-ray diffraction. A transition from the monoclinic (I) γ-phase to the triclinic δ-phase after moderate mechanical treatments has been observed for untreated powder, just what happens when the same samples are rapidly cooled to low-temperature. Evidences of the low temperature monoclinic (II) polar ε-phase have been found at room temperature in samples after a stronger milling treatment. The sequence of the low-temperature phase transitions appears to be strongly dependent on the mechanical history of the powders. A new low-temperature N-phase has been observed below about 200 K in different samples: it is the main phase in commercial untreated powders, having the monoclinic (I) γ-phase at room temperature, but constitutes only a small fraction in moderately treated powders, having the triclinic δ-phase at room temperature.

INTRODUCTION

Different crystal phases of tungsten trioxide (WO_3) have been investigated using several experimental techniques in the past years (1–13), and theoretical calculations have been developed to explain the polymorphism of this compound (14). The interplay between the lattice phonons and the electronic structure of WO_3 results in the occurrence of several phases, starting from low symmetry triclinic or monoclinic phases up to the tetragonal phase.

On the basis of reported experimental data, the following sequence of crystal phases, in order of increasing temperature, is presently accepted: monoclinic (II) polar or ε-phase with space group Pc (C_s^2), from 5 to 278 K (11); triclinic or δ-phase, $P\bar{1}$ (C_i^1), from 248 to 290–300 K (1, 7, 9, 11); monoclinic (I) or γ-phase, $P2_1/n$ (C_{2h}^5), from 290–300 K to 600 K (1–3, 9); orthorhombic $Pmnb$ (D_{2h}^{16}), from 600 to 1010 K (6); tetragonal $P4/nmm$ (D_{4h}^7), from 1010 K (10) to the melting temperature 1746 K. Recent low-temperature (from 5 to 250 K) neutron diffraction studies, performed by Salje *et al.* (11) on finely ground powders, confirmed the ε-to-δ-to-γ phase transition sequence for increasing temperature and did not evidence any other phase below 220 K.

Such sequences of low-temperature crystal phases occur for single or polycrystals showing yellowish green color, associated with a charge carrier concentration of the order of 10^{18} cm^{-3} (13, 15). However, the preparation route, the exact stoichiometry, the presence of impurities and the mechanical treatments are known to modify it. In many cases, the WO_3 powdered samples exhibit at room temperature (RT) the coexistence of δ and γ phases. At lower temperature, for some samples, the expected transition to the ε-phase (monoclinic (II) polar) is not observed (4, 16). Furthermore, microcrystals of very small size (below 100 nm), obtained via evaporation techniques, exhibit at low temperatures Raman spectroscopic indications of new phase, characterized by a relevant downshift of the stretching modes of W–O bonds (17, 18), usually found at about 715 and 805 cm^{-1} in δ- and γ-phases.

In general, the high temperature phases show a good reproducibility of the results and low hysteresis effects; the phase sequence does not depend on impurity content or mechanical treatments. In contrast, quite different behaviors are reported at RT and below depending on the type of samples and on their mechanical and thermal history.

The vibrational spectroscopy is a powerful tool for following the phase transitions in tungsten trioxide, providing complementary information to the one collected by diffraction techniques. Until now, Raman and IR spectroscopic studies have been widely used for the phases close to RT (19, 20), but only microcrystal studies have been carried out, to our knowledge, for very low-temperatures (17, 18), and no comprehensive Raman investigation of the role of mechanical treatments in the phase transition sequence has been carried out.

0022-4596/99 $30.00

In this work a comparative study of the low-temperature crystal phases of tungsten trioxide is carried out on powder samples that underwent different milling processes and have at RT γ- or δ-phase. For this reason, a preliminary investigation is made on the γ-to-δ phase transition induced by both mild mechanical treatments and fast thermal cooling.

EXPERIMENTAL

Sample Preparation

The starting material for the present study is commercial stoichiometric WO_3 powder ("Reahim," Russia) for optical industrial applications, with a nominal purity of 99.998% (percentages of present impurities have the following upper limits: $V < 5 \times 10^{-4}$; $Fe < 5 \times 10^{-4}$, $Co < 1 \times 10^{-4}$, $Mn < 1 \times 10^{-4}$, $Cu < 1 \times 10^{-4}$, $Ni < 1 \times 10^{4}$, $Cr < 5 \times 10^{-4}$). The stoichiometry of the powder WO_3 (with an oxygen content at least higher than 2.999) is indicated by pale yellow color and was controlled by EPR measurements down to liquid helium temperature. No EPR signals from impurities or W^{5+} defects were found (21). Preliminary measurements, performed with different excitation laser lines, indicate no luminescence in the visible wavelengths and no vibrational bands related to surface water or OH groups. Before the spectroscopic investigations this powder had a long storage time (order of years) in equilibrium with atmospheric oxygen, and its yellow color remained stable (in fact, other experiments on purposely reduced powder samples, via milling or other treatments, showed that long interaction with air at RT induced a reoxidation of the powders (22)). An inspection by the optical microscope indicates that these powders have an average grain size of the order of micrometers.

From this powder three different sets of samples have been obtained and studied separately. The first sample was the as-purchased powder, in the following identified as "virgin powder." A second set of samples was produced from the commercial powder which underwent a mild milling procedure, consisting of a manual compression in a mortar of agate for a few minutes. The structural differences between these materials are demonstrated by our XRD and Raman measurements, discussed later; in the following this second kind of powder will be labeled as "treated powder." A third set of samples was produced from the virgin powder via strong mechanical treatments by using a ball milling machine Retschmuele, with three balls of agate having diameters between 0.5 and 1 cm and weight between 0.17 and 1.09 g, working at a frequency of the order of 1 Hz (50–70 cycles per minute) for different times, ranging from a few minutes up to 21 h. In the present work we focus the attention on the samples that underwent 1 h milling, which will be referred to as "ground powders."

Experimental Set-up

The samples were analyzed by powder X-ray diffraction (XRD) and Raman spectroscopy. The samples for XRD were prepared by deposition on a Millipore filter of the powder from an aqueous suspension driven by a vacuum pump. A Bragg-Brentano X-ray diffractometer, made by ItalStructures, working with Cu$K\alpha$ radiation was used. The X-ray diffractograms were recorded at RT in the angle range $2\theta = 20$–65° and a step $\Delta(2\theta) = 0.05^\circ$.

For the Raman spectroscopic measurements the most successful sample preparation method consisted of a deposition on a microscopy cover glass of some droplets of a suspension of WO_3 powders in acetone. After the necessary time for solvent evaporation the deposited powders showed a good adhesion to the substrate and allowed for a good Raman signal detection. The RT Raman measurements have been carried out in back-scattering geometry using a micro-Raman setup, consisting of an Olympus microscope (Model BHSM-L-2), mounting an $80\times$ objective with a $N_A = 0.75$ numerical aperture coupled to a 1-m focal length double monochromator Jobin-Yvon (Ramanor, Model HG2-S) equipped with holographic gratings (2000 grooves/mm). The spectra were excited by the 530.9-nm line of a Krypton laser, which was operated so that the power entering in the microscope was maintained below 10 mW. The spectral resolution was of the order of $3\ cm^{-1}$. The scattered radiation was detected by a cooled (-35°C) photomultiplier tube (RCA, Model C31034A-02), operated in photon counting mode. The signal was stored into a multichannel analyzer and then sent to a microcomputer for the analysis. For the temperature dependence study, the experimental setup was set in the standard macro-Raman configuration, and a right angle scattering geometry was adopted. In this configuration the spectra were excited by the 514.5-nm line of the argon laser used, with a nominal power of 20 mW at the cryostat window. For low temperature range (30–270 K) a liquid helium flux cryostat has been used, and a small glass with a proper amount of deposited WO_3 powders was used as sample holder.

The nominal temperature values are given by the sensor of the temperature controller, but the laser irradiation during the Raman measurements can induce a local heating at the observed spot. To have a more realistic information on the temperature value, the Stokes/anti-Stokes intensity ratio has been studied for each spectrum for the Raman modes in the range 20–$200\ cm^{-1}$. Thus the obtained temperatures have an error of about ± 5 K.

RESULTS AND DISCUSSION

Phase Transition Induced by Mechanical Treatments

It is reported that the sequence of phase transitions between the low symmetry crystal structures of WO_3 depends

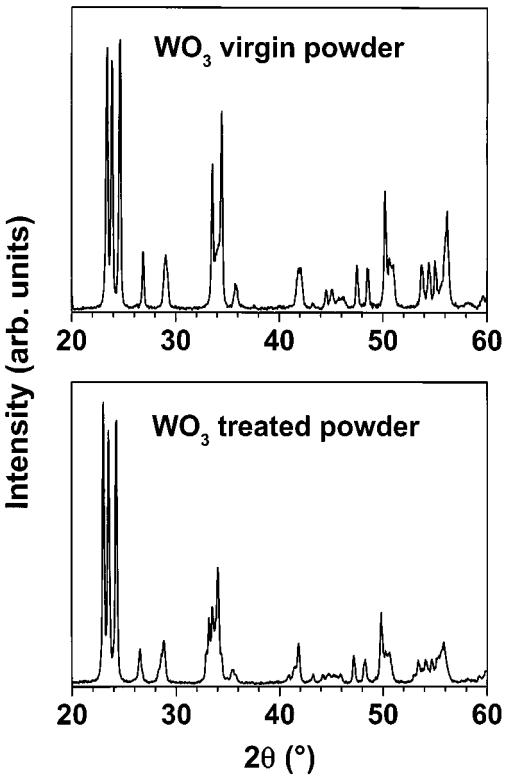

FIG. 1. XRD spectra of WO_3: monoclinic (I) γ-phase "virgin powder" (top); triclinic δ-phase "treated powder" (bottom).

on the crystal growth history (4, 5), indicating that the equilibrium of the crystal phases should be sensitive to the mechanical perturbations and to the stoichiometry (which affects the charge carrier concentration). In our present study, structural transformations are observed as a consequence of simple mechanical treatments, like milling for variable times, but also after manual compression for relatively short times of the order of minutes. A transition in the WO_3 powder from γ (monoclinic) to δ (triclinic) structure, under weak milling treatment, can be inferred from small modifications of the XRD patterns, as shown in Fig. 1. The XRD patterns given by the virgin powder (having mainly γ-phase) and the treated samples (having mainly δ-phase) are quite similar, because of the small differences between the lattice parameters of the two phases. However, the changes in the diffraction peaks, mainly at about $2\theta = 34^\circ$, allow for a clear attribution of the different samples to different crystal structures. The transformation induced in such a way is stable for a time scale of months, and it can be reversed only by thermal annealing at high temperatures (at least $T > 570$ K).

The Raman spectroscopy can give a clearer evidence of the phase changes and allows to follow the different steps of the transformation by analyzing the evolution of lowest frequency peaks (up to 100 cm^{-1}) of the Raman spectra (22). These peaks correspond to lattice modes of librational nature and are noticeably affected by the transitions between the low symmetry phases of WO_3, which involve mainly collective rotations of the basic [WO_6] octahedral units (7, 10). The Raman spectra show different features in the γ- and δ-phases (4, 5, 22): in particular the 34 cm^{-1} peak is typical of monoclinic γ-phase, while the 43 cm^{-1} peak characterizes the triclinic δ-phase.

Figure 2 shows an interesting parallel evolution for the Raman spectra of γ-phase virgin powder, which transforms into the δ-phase by effect of mechanical compression (a) or fast thermal cooling (b). Figure 2a reports various spectra in the range 20–100 cm^{-1} for samples, which underwent cumulatively increasing times of grinding up to 2 min. Such evolution for ground WO_3 powders, reflecting the gradual transformation from γ- to δ-phase, is quite similar to that observed at RT for powder samples after different and cumulative cooling times (from a few minutes up to about 2 h) in liquid nitrogen (Fig. 2b).The occurrence of the δ-phase at RT after preliminary cooling in liquid nitrogen has been also observed in neutron diffraction study (9). The final δ-phase appears to be well defined both for XRD (Fig. 1) and Raman spectroscopy (Fig. 2).

A different phenomenology occurs when the mechanical treatments increase in both strength and duration. Maintaining always a fixed milling frequency of about 1 Hz, the effect of increasing grinding time has been analyzed: for treatments of the order of 1 h a change of color was observed from the pale yellow of the monoclinic (I) or triclinic powders toward a greenish color; a bluish coloration has been reached by increasing the time of milling up to many hours (22).

The structural evolution and the average crystal size for increasing milling time can be observed through the XRD spectra. The analysis of XRD patterns for ground powders samples, based on the Scherrer method (23), shows that upon milling a decrease of the crystallite size occurs by about four to five times for 1 h treatment, leading to the broadening of the diffraction lines.

After a first transformation into the δ-phase, observed for mild mechanical treatments, at some step of the structural evolution (after about 1 h milling) new Raman peaks appear at 143, 643, and 680 cm^{-1} (Fig. 3): they correspond to the ones of the low temperature monoclinic (II) ε-phase (5). The occurrence of the ε-phase in these *ground powders* is also supported by XRD measurements, as shown in Fig. 4, where a new diffraction peak appears for $2\theta = 24^\circ$. To our knowledge, a Raman evidence of ε-phase at RT was previously reported for WO_3 microcrystals of size below 100 nm (17,18). On the other hand, the characteristic peaks of ε-phase has not been detected in the low-temperature spectra collected on the virgin or moderately treated powders in the present work (see below).

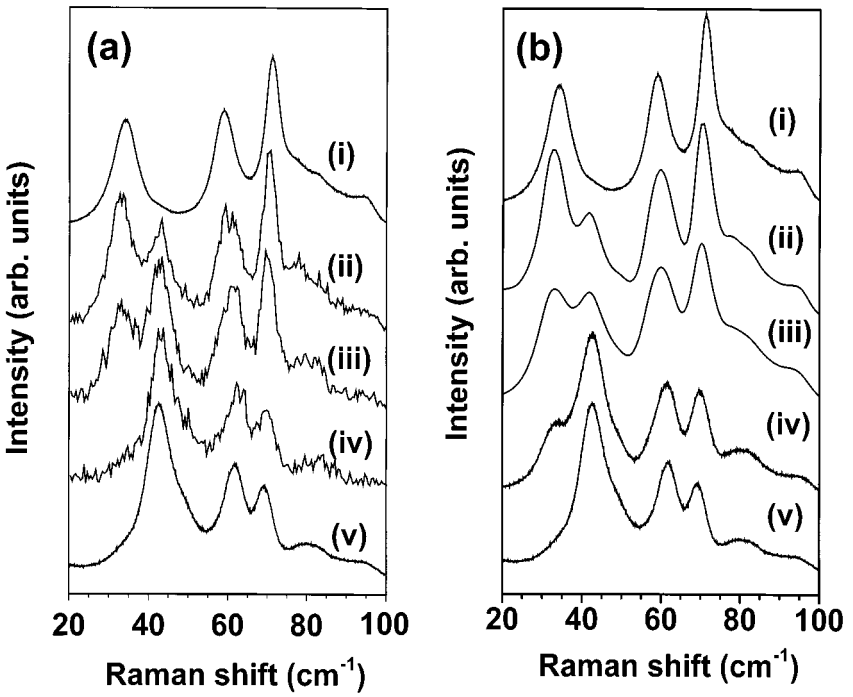

FIG. 2. (a) Low-frequency Raman spectra of WO_3 virgin powder samples underwent cumulative mechanical pressure treatments for short times: (i) starting virgin powder (γ-phase); (ii) after 5 s compression; (iii) after 10 s compression; (iv) after 120 s compression; (v) reference treated powder sample, after 10 min moderate milling (δ-phase). Note the strong rearrangement of the low-frequency spectra since the early steps of pressure application. (b) Low-frequency Raman spectra collected at RT on WO_3 virgin powder underwent fast cooling by immersion in liquid nitrogen and kept there for different times: (i) starting virgin powder; (ii) after 5 s immersion in LN2; (iii) 1 min immersion; (iv) 10 min immersion; (v) 2 h immersion. Also here strong spectral changes occur, similar to those reported in (a).

Low-Temperature Phases

A direct comparative study has been made between the virgin powder and the treated powder, which have been mounted in the cryostat and cooled, following the same experimental procedure.

The virgin powders have been cooled in the liquid He flux cryostat down to $\sim$10 K, in about 3 h; thereafter several Raman spectra have been recorded, each one after some stabilization time, for increasing temperatures, starting from a nominal value of 18 K upward.

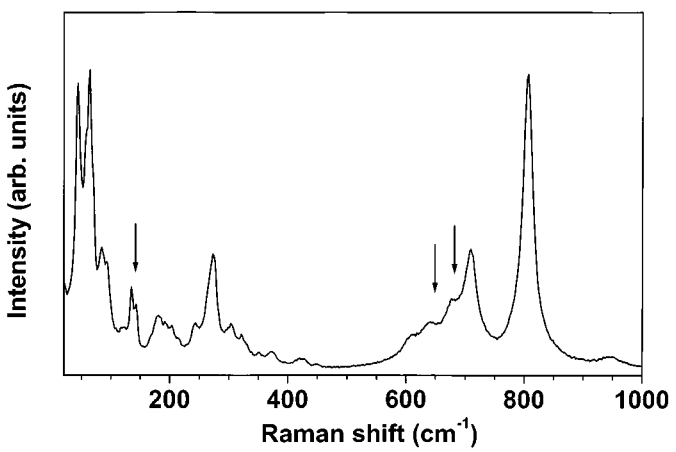

FIG. 3. Raman spectrum of WO_3 ground powder after 1 h milling. Arrows indicate the typical features of the monoclinic (II) ε-phase at 143, 643, and 679 cm^{-1}.

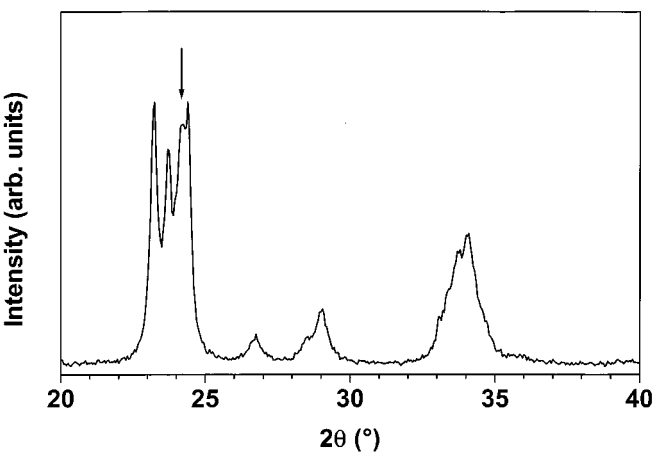

FIG. 4. XRD pattern of WO_3 ground powder after 1 h milling. The peak at $2\theta \approx 24^\circ$, related to the monoclinic (II) ε-phase, is indicated by an arrow.

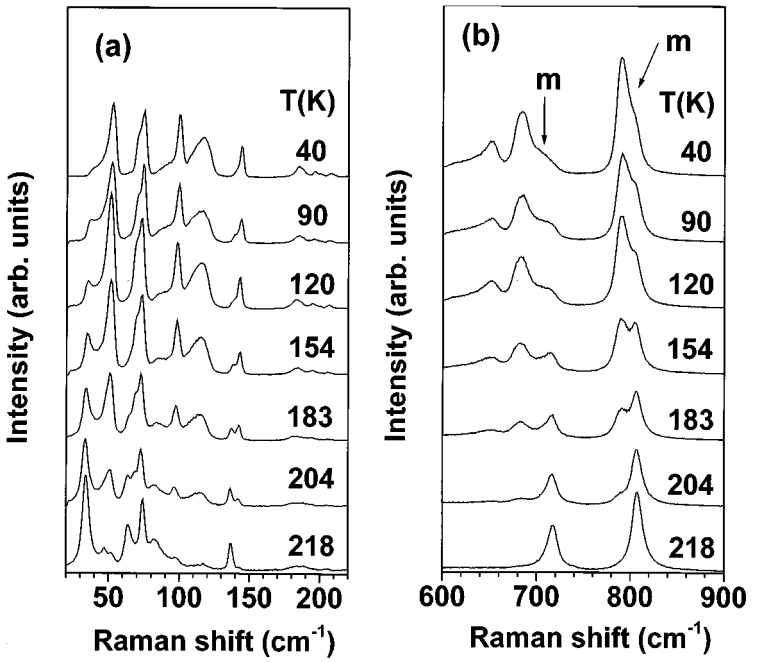

FIG. 5. Low-temperature evolution of the low-frequency modes (a) and high-frequency stretching modes (b) in Raman spectra of WO_3 virgin powder. Shoulders attributed to the residual monoclinic (I) γ-phase are labeled by "m" in the lowest temperature spectrum. The reported temperatures are estimated from the Stokes/anti-Stokes ratio.

As can be seen in Fig. 5, a great change of the spectral shape occurs in the explored temperature range, but this spectral evolution can be interpreted as the transformation between two phases only. At the lowest temperatures the modes of the monoclinic (I) γ-phase (stable at RT) survive as weak features or shoulders on stronger bands attributed to a new phase (N-phase). These characteristic modes of the N-phase are strongly dominant below 120 K. The most evident peaks are at 684 and 790 cm^{-1}, but other peaks are also observed in the low frequency range. Some modes having quite close frequencies were previously observed at low temperature in WO_3 microcrystals (17, 18), grown by an evaporation method. In Table 1 all the modes, observed in the present study are listed for γ- and δ-phase at RT and for new N-phase at 40 K.

The slow transformation from the N-phase to the γ-phase appears to be diffuse in a broad temperature range: this behavior can be qualitatively depicted as a phase equilibrium with a temperature dependent constant, so that the WO_3 powders evolve from a composition with prevalent N-phase at about 40 K to the pure γ-phase at RT. Note that the modes typical for the N-phase are observable up to about 200 K. This transition is well reversible and reproducible: in fact, a quite similar behavior is observed in a second set of measurements on the same sample, stored for 2 days at RT, and cooled down again to 10 K, with the temperature going upward along all the measurements.

Another point to be remarked in the low temperature Raman spectra of the *virgin* powder (Fig. 5) is that there is no indication of the monoclinic (II) polar ε-phase, previously reported by Salje *et al.* in single crystals at $T \sim 230$ K (4, 5) and in polycrystalline sample at $T < 220$ K (11). This absence, however, has been already reported in other studies on powder samples (4, 16). Moreover, in the present measurements no evidence was also found for the expected transition to the triclinic δ-phase. It has been observed, on the contrary, at low temperatures in most previous works (4, 5, 10). In our samples the δ-phase is obtained and remains stable at RT only after moderate milling or after fast cooling in liquid nitrogen.

It is interesting to compare these findings with the previous observation in microcrystals (17, 18). In that case the competing phases were mostly the ε- and N-phases, and the ratio between them depended on the evaporation conditions. However, the Raman amplitude ratio for the respective peaks indicates that the maximum obtained percentage of the N-phase was comparable to that reported in the our study for the virgin powders.

The treated powder samples were studied in a manner similar to that used with the virgin ones: they were cooled in the liquid He flux cryostat down to minimum attainable temperature (~ 10 K), and the Raman spectra were recorded thereafter at increasing temperatures. For these measurements, the difference between the nominal

TABLE 1
Raman Bands for New (N), Triclinic, and Monoclinic (I) Phases of WO_3

N-phase		Triclinic		Monoclinic (I)	
Wavenumber (cm^{-1})	Relative amplitude	Wavenumber (cm^{-1})	Relative amplitude	Wavenumber (cm^{-1})	Relative amplitude
52	44	43	118	34	61
70	29	48	66	59	65
74	40	62	80	71	90
99	37	70	67	78	41
116	24	82	31	83	35
144	18	96	20	95	24
185	7	121	12	134	40
196	4	137	36	167	6
208	3	178	14	178	7
254	3	186	16	187	9
275	56	193	14	205	6
289	3	217	9	220	7
332	8	244	15	240	5
348	3	265	20	273	45
358	2	277	41	294	6
382	4	296	8	326	13
400	3	316	8	331	9
435	4	324	12	348	4
615	11	332	9	378	3
651	28	354	6	397	3
684	54	380	4	417	3
790	100	419	3	437	4
		431	4	448	4
		451	2	576	6
		609	12	639	6
		712	49	717	60
		808	100	807	100

Note. Wavenumber and relative amplitude (with respect to the highest frequency stretching mode of any phase, whose amplitude is fixed to 100).

temperature given by the sensor and the effective one estimated via the Bose-Einstein factor calculation is larger, in particular at the lowest temperatures; this fact can be partially attributed to different thermal conductivity of the smaller grains.

A set of Raman spectra for treated powders, measured at temperatures up to 260 K, is shown in Fig. 6. It is quite evident that no dramatic change of the spectral shapes occurs in the explored temperature range, besides the usual broadening of the peaks with temperature, in particular for the bands at 81, 241, and 610 cm^{-1}. Even at the lowest temperature (70 K) the main spectral pattern corresponds well to that of the triclinic δ-phase observed at RT.

In the treated powders no clear spectroscopic evidence of the ε-phase was found: only very weak features appear in the lowest temperature spectra at about 750 and 650 cm^{-1}, but their intensities are comparable to the noise level. On the other hand, the spectroscopic evidences for the N-phase are certainly detectable, but they are much weaker than in virgin powders: the presence of the N-phase appears as the asymmetry of the low frequency side of the 712 and 808 cm^{-1} stretching modes, marked by arrows in the lowest temperature spectrum of Fig. 6b. These shoulders are consistent with the satellite bands at 687 and 787 cm^{-1}, reported by Hayashi *et al.* (17, 18) at low temperatures on microcrystalline samples, and with the bands well observed in the virgin powder sample (Fig. 5 and Table 1). Their low relative intensity indicates that the fraction of the N-phase in the treated powder is much smaller than in the case of the virgin powder.

A quantitative estimation cannot be made in both cases, because different modes can have different temperature dependence of the Raman tensor components, and the frequency dependence of the Bose-Einstein factor must be also considered. In addition, the width of the bands and their small separation do not allow unambiguous assignment of the various modes via fitting procedure. However, direct observation of the spectra, reported in Figs. 5 and 6, reveals without any doubt the strong transformation upon cooling toward the N-phase for the virgin powders (from γ- to N-phase), and the much weaker transformation for the treated powders (from δ- to N-phase).

The surface-to-volume ratio (i.e., the microcrystal size) together with the temperature change have been invoked to explain the stability of the different crystal structures (17, 18). The broad temperature range of the transition to the N-phase suggests a size dependence of the transition temperature. The present observations show a much higher fraction of N-phase for the samples of virgin powders, which have surely grains of larger size with respect to the treated powders, that is in agreement with the previously studied microcrystal size dependence of the transition (17, 18). However, the findings of the transition to N-phase in the *virgin* commercial powders, having a much greater grain size than evaporated microcrystals, makes it possible to rule out the hypothesis that the N-phase could be a peculiar characteristic of microcrystalline samples. Moreover, other variables besides the crystal size, like the stress and carrier concentration (connected to substoichiometry), also play an important role in driving such transition and have to be carefully considered.

The anomalous low value of the stretching frequency in the N-phase Raman spectrum (790 cm^{-1} against more than 800 cm^{-1} for all the other phases) suggests a more relaxed structural configuration, which cannot be induced by simple lattice parameter contraction, usually obtained by temperature reduction or high-pressure application. In fact, a high-pressure Raman investigation (24) shows that a pressure of about 0.15 GPa promotes the γ-to-δ transition, a stronger pressure of 0.2 GPa promotes the transition to the ε-phase, but no other phases are observed for pressures up to 1.4 GPa. A more recent high-pressure diffraction study (25), extended up to about 5 GPa, confirms that only the ε-phase

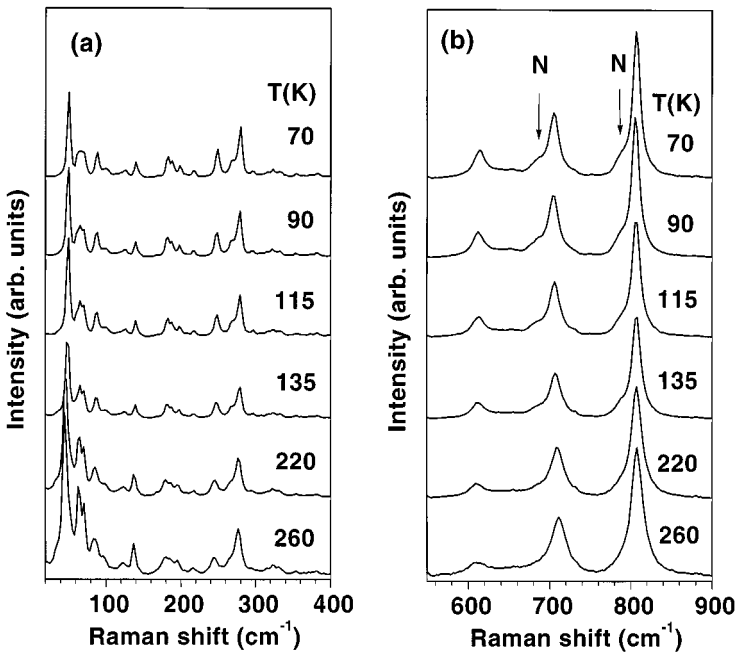

FIG. 6. Low-temperature evolution of the low-frequency modes (a) and high-frequency stretching modes (b) in Raman spectra of WO_3 treated powder. Shoulders attributed to the N-phase are labeled by "N" in the lowest temperature spectrum. Temperature values are obtained from the Stokes/anti-Stokes ratio.

exists in the measured pressure range. Thus the N-phase and the ε-phase represent opposite evolutions of the crystal structure, and we could expect that conditions promoting the transition to the N-phase inhibits the transition to the ε-phase and vice versa.

By assuming that pressure effects are comparably reproduced by the amount of cumulative stress, we can also explain the γ-to-δ phase transition, easily obtained via application of a low amount of stress, which can be produced by mild milling treatment or also by a fast cooling process. Furthermore, the application of larger amount of stress can justify the observation of a small fraction of powders going into the ε-phase at room temperature after 1 h milling treatment. The occurrence at room temperature of the ε-phase has been observed also in the evaporated microcrystal of smaller size (17, 18), and even for that finding a similar explanation based on the crystal stress can be proposed.

We can also speculate about known relationship between carrier density and structural transitions of WO_3 crystals. For example, the *n*-type WO_3 crystals show carrier concentration dependence of the ε-phase stability. As shown by Salje *et al.* (11), the free carriers are localized at low temperature in (bi-)polaronic states associated with a local lattice deformation.

For simple symmetric structures, the presence of polarons introduces a strain associated with the anions displacements of expansive type. Among the WO_3 compounds, tungsten bronzes constitute a good example of symmetric structure, and, in fact, some insight on the amount and the character of the strain due to polarons is given by XAFS studies of intercalated H_xWO_3 oxides: they have shown a local expansion of ~ 0.1 Å for the oxygens around tungsten ions in $[W^{5+}O_6]$ octahedra (26).

However, the complex interplay of various lattice potential terms can lead to a different type of deformation. Theoretical calculations of the polaron stability (27), based on the study of the competing elastic and electron–phonon terms of the potential, have been carried out for the low symmetry phase of tungsten trioxide. The calculated polaronic displacements (27) in the monoclinic (I) lattice (the γ-phase) were found to be compressive for all the atoms around the polaronic W^{5+} center. This is due to the negative sign of the electron–phonon interaction term, induced by the low symmetry of the anions arrangement around the W^{5+} ions. The prediction of this anomalous behavior has been made both for single polarons as well as for bipolarons (27) and seems to be consistent with our hypothesis of low temperature structural evolution presented below.

In fact, the simple empirical evidence of high-pressure studies (24, 25) suggests that the ε-phase is stabilized at high pressures. Therefore it seems reasonable to postulate that a transition to a compressed phase can be obtained either by using high external pressures (simulated in some way by the grinding treatments) or by cumulating the internal compressive strain due to polarons.

We suggest that the ε-phase is favored by the total strain generated by (bi)polarons when they reach a sufficient concentration, equivalent to the application of high pressure. Thus the evolution of WO_3 toward either ε-phase or N-phase can be determined also by the carrier concentration, associated with oxygen deficiency. In fact, slightly defective WO_{3-x} samples show the transition to the ε-phase (8, 13), while the N-phase seems to be characteristic of crystals having minimum amount of stress and very low carrier concentration. This hypothesis must be confined to the range of small and very small charge carrier concentration, because it is known that in highly reduced samples a metallic like conductivity occurs and the stability of low temperature ε-phase is destroyed (28). Finally, the observed crystal size dependence of phase transitions in our powders having different grain sizes can be correlated with the presence of the localized and nonlocalized charge carriers which originate at the reduced free surface of WO_3 crystals (29).

CONCLUSIONS

The present investigations of the tungsten trioxide commercial powders below room temperature, down to about 40 K, show different phase transition sequences with respect to the previous studies (4, 5, 11) and, in particular, the occurrence of a diffuse transition into the new N-phase. The low temperature crystal structures of the powder samples are strongly influenced by the different mechanical history of the samples, and the kinetics of the transitions appear to be relevant. Such behavior reveals the occurrence of processes difficult for a description within the thermodynamic equilibrium framework. The diffuse transition to the N-phase, in the wide temperature range 40–200 K, appears as the most relevant phenomenon in the low-temperature transformation of WO_3 virgin powder samples analyzed in the present work.

The Raman spectroscopic evidences of the low temperature evolution studied here for different powder samples can be summarized as follows:

(i) Virgin powders of large grain size with no accumulated stress and having γ-phase at RT transform increasingly into the N-phase upon cooling. The transition to the triclinic δ-phase, reported for other samples (1, 7, 9, 11) is not observed.

(ii) Only a small fraction of the treated powders, having small grain size and mechanically stressed before the cooling process, transforms at comparable temperatures into the N-phase. In this case, the starting triclinic δ-phase, obtained by moderate milling at room temperature, remains dominant even at the lowest temperatures.

(iii) No clear spectroscopic evidence of the transition to the ε-phase, reported by Salje *et al.* for single crystals at $T \sim 230$ K (4, 5) and polycrystalline samples at $T < 220$ K (11), is observed in both virgin and treated powders upon cooling.

(iv) In contrast, a transition to the ε-phase is observed for a small fraction of the powder samples at room temperature after 1 h milling. For longer milling times the broadening of the peaks does not allow to discriminate the crystal phases present in the powder samples.

It is noticeable, for the powder samples used in the present work, that the low-temperature phases, such as the δ-phase and the ε-phase, are not obtained by cooling in equilibrium conditions, as usually reported in most of the existing literature (1, 7, 9, 11), but rather by more or less prolonged mechanical stress at room temperature. However, this fact seems to be consistent with high-pressure measurements, showing the γ-to-δ phase transition for relatively low applied pressures and the transition to the ε-phase for higher pressures (24, 25). In fact, the δ-phase has been also observed in the virgin powders after fast cooling by immersion in liquid nitrogen. On the contrary, a slower cooling rate, given by the helium flux cryostat, leaves the virgin powders into the γ-phase, until a new N-phase, never found previously in macroscopic crystals (4, 5, 11), appears below 200 K and becomes dominant at the lowest temperatures. It is worth remarking on the dependence of the transition on the cooling kinetics.

Obviously the Raman spectral evolution alone cannot provide a satisfactory description of the polymorphysm of WO_3, in particular about the space group of the N-phase, and a clear crystallographic definition can be given only by low-temperature XRD measurements. Nevertheless, the observed Raman spectrum of the N-phase, with its unique lowering of the highest frequency stretching modes, is a good marker of this phase, allowing its fast recognition in different samples.

The understanding of the new N-phase and the transitions between the different observed structures should take into account the interplay of stress, crystal size (surface effects) and carrier concentration. In our opinion, further studies, focused on the interaction of charge carriers responsible for the electronic properties of the material (11, 13) with the low-temperature structural phase transitions, are necessary.

ACKNOWLEDGMENTS

A.K. and J.P. thank the Centro CNR-ITC di Fisica degli Stati Aggregati ed Impianto Ionico (Trento) and the Università di Trento for hospitality and financial support.

REFERENCES

1. S. Tanisaki, *J. Phys. Soc. Jpn.* **15,** 566 (1960).
2. B. O. Loopstra and P. Boldrini, *Acta Crystallogr. B* **21,** 158 (1966).
3. B. O. Loopstra and H. M. Rietveld, *Acta Crystallogr. B* **25,** 1420 (1969).
4. E. Salje and K. Viswanathan, Acta *Crystallogr. A* **31,** 356 (1975).
5. E. Salje, *Acta Crystallogr. A* **31,** 360 (1975).
6. E. Salje, *Acta Crystallogr. B* **33,** 574 (1977).

7. R. Diehl, G. Brandt, and E. Salje, *Acta Crystallogr. B* **34,** 1105 (1978).
8. T. Hirose, *J. Phys. Soc. Jpn.* **49,** 562 (1980).
9. P. W. Woodward, A. W. Sleight, and T. Vogt, *J. Phys. Chem. Solids* **56,** 1305 (1995).
10. K. L. Kehl, R. G. Hay, and D. Wahl, *J. Appl. Phys.* **23,** 212 (1952).
11. E. K. H. Salje, S. Rehmann, F. Pobell, D. Morris, K. S. Knight, T. Herrmannsdörfer, and M. T. Dove, *J. Phys.* C: *Condens. Matter* **9,** 6563 (1997); E. Salje, Ferroelectrics **12,** 215 (1976).
12. E. Iguchi, H. Sugimoto, A. Tamenori, and H. Miyagi, *J. Solid State Chem.* **91,** 286 (1991).
13. I. Lefkowitz, M. B. Dowell, and M. A. Shields, *J. Solid State Chem.* **15,** 24 (1975).
14. J. B. Goodenough, *Prog. Solid State Chem.* **5,** 145 (1971).
15. J. M. Berak and M. J. Sienko, *J. Solid State Chem.* **2,** 109 (1970).
16. A. Anderson, *Spectrosc. Lett.* **9,** 809 (1976).
17. M. Arai, S. Hayashi, K. Yamamoto, and S. S. Kim, *Solid State Commun.* **75,** 613 (1990).
18. S. Hayashi, H. Sugano, H. Arai, and K. Yamamoto, *J. Phys. Soc. Jpn.* **61,** 916 (1992).
19. E. V. Gabrusenoks, *Sov. Phys. Solid State* **26,** 2226 (1984).
20. M. F. Daniel, B. Desbat, J. C. Lessegues, B. Gerand, and M. Figlarz, *J. Solid State Chem.* **67,** 235 (1987).
21. J. J. Purans and P. D. Cikmach, "Proceedings, All Union Conference on Physics of Oxide Films," p. 51. Petrozavodsk, 1982. [in Russian]
22. E. Cazzanelli, G. Mariotto, C. Vinegoni, A. Kuzmin, and J. Purans, *Proc. Electrochem. Soc.* **96**-24, 260 (1996); A. Kuzmin, J. Purans, E. Cazzanelli, C. Vinegoni, and G. Mariotto, *J. Appl. Phys.* **84,** 5515 (1998).
23. J. I. Langford and D. Louër, *Rep. Prog. Phys.* **59,** 131 (1996).
24. E. Salje and G. Hoppman, *High Temp. High Pressures* **12,** 213 (1980).
25. Y. Xu, S. Carlson, and R. Norrestam, *J. Solid State Chem.* **132,** 123 (1997).
26. A. Kuzmin and J. Purans, *J. Phys.*: *Condensed Matter* **5,** 2233 (1993).
27. E. Iguchi and H. Miyagi, *J. Phys. Chem. Solids* **54,** 403 (1993).
28. E. Salje, A. F. Carley, and M. W. Roberts, *J. Solid State Chem.* **29,** 237 (1979).
29. F. H. Jones, R. A. Dixon, and A. Brown, *Surf. Sci.* **369,** 343 (1996).